Available online www.jocpr.com

Journal of Chemical and Pharmaceutical Research, 2019, 11(10):1-12

Research Article

ISSN: 0975-7384
CODEN(USA): JCPRC5

Molecular Interaction and Binding Studies of Azabicyclononane Derivatives with Bovine Serum Albumin (BSA)

Bhavapriya R[1], Venkatraman M[1*] and Sathiyanarayanan KI[2]

[1]*School of Biosciences and Technology, Vellore Institute of Technology Vellore, India*

[2]*School of Advanced Sciences, Vellore Institute of Technology Vellore, India*

ABSTRACT

Azabicycle ABN (2,4-Diaryl-6,7-benzo-3-azabicyclo[3.3.1]nonan-9-ones) is a well-documented alkaloid for its wide range of biological applications and as a building block for various drug molecules. For our studies Azabicycle derivatives (5a, 5b and 5d) have been synthesized based on mannich approach, where5a is methyl, 5b is methoxy and 5d is fluoro substituted derivatives. The main aim of this study is to characterise the interaction between Bovine serum albumin (BSA) with azabicycle derivatives. BSA is used since albumin is the copious protein found in blood plasma and commonly used to investigate interaction studies of various drug molecules, so far nanoparticles like silver, iron, zinc, titanium dioxide nanoparticles etc., have been studied and some chemically synthesized metal complexed drug molecules has been established. In this study, we analyse the interaction of various concentration (6.25, 12.5, 25 and 50 µM) of azabicycle derivatives with BSA. To facilitate the preclinical development further, the interaction between ABN and BSA was studied using UV spectroscopy, Dynamic light scattering (DLS) fluorescence quenching and Fourier transform infrared spectroscopy (FTIR). The excitation wavelength 280nm of UV spectroscopy shows the interaction of compound. In DLS average size of the particles increased when interacted with BSA. FTIR peaks further confirm the interaction of ABN-BSA complex. The excitation wavelength of quenching analysis of ABN-BSA compound proves the interaction. Hence BSA has significantly decreased when increase in concentration of ABN compounds. This study reveals the detailed evaluation of ABN-BSA complex formation.

Keywords: Azabicycle; Bovine serum albumin; Interaction; Various concentration; ABN-BSA complex

---

INTRODUCTION

Azabicyclononane (*2, 4-Diaryl-6, 7-benzo-3-azabicyclo [3.3.1] nonan-9-ones*) derivatives are found as naturally occurring alkaloids in plant species especially Aconitum and Delphinium plants. Azabicyclononane (ABN) contains piperidin moiety, which is a well-documented alkaloid for its wide range of biological applications and as a building block for various drug molecules [1]. Here in this work, Azabicyclononane was synthesized based on mannich

approach. Usually mannich reaction is used in to synthesize of natural and pharmaceutical products such as antitumor agent like curcumin, taxol etc and involves in the condensation of amine, aldehyde and ketone group in acidic medium [2]. Figure 1 depicts the general synthetic reaction scheme of mannich reaction.

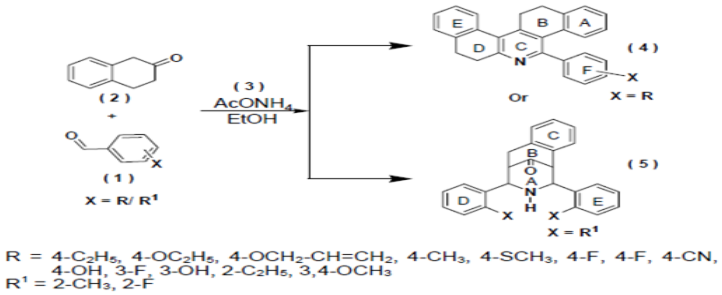

Figure 1. Mannich based approach synthesis and structural details expressed

Wide varieties of Phenanthridine have toxic effects and their binding characteristics are well reported, however in case of azabicyclonanane only few reports are found, and thus its toxic effects are not clear yet [3]. Interaction reports with serum proteins were also not reported. Azabicyclononane compound interacts with proteins and dopamine like receptors, when it enters in human system ultimately decides the level of toxicity it induces. Only few reports discuss about Azabicyclononane binding activity particularly in dopamine receptors [4].

Serum albumin is the abundant protein found in blood plasma. Interaction studies with protein gives better insight on absorption, distribution and metabolism of drug molecules. Binding affinity towards proteins like HSA and distribution of drug compound based on charge present in protein. The binding characteristics with albumin proteins help in studying the designing of dosage and to understand pharmacokinetic property of the drug compound [5-7]. Usually Bovine serum albumin (BSA) can be used commonly to study toxicity of various drug compounds due to its structural homology (76% similar to Human serum albumin (HSA)) [5].

Here in this work, we report binding characteristics of ABN interaction with BSA. The protein conformation, kinetics and adsorption were analyzed by UV-Visible spectrophotometer, dynamic light scattering, FT-IR spectroscopy and Fluorescence quenching. FT-IR spectroscopy was applied to characterize ABN and BSA interaction.

For instance quenching conformational changes like side on or end on interaction in the molecules of ABN to BSA. As this study will be very useful in drug design studies and similar studies can be done for other metallic and chemically synthesized drug molecules [6].

Here, we analysed the changes in BSA characteristic peaks before and after the interaction. FT-IR was used to characterize the bindings of Azabicycle derivatives at α-helix or β-sheet of BSA protein. Interaction of ABN and BSA increases protein size and was monitored using DLS analysis. Further, interaction can be quantified through quenching characteristics of aromatic chromophores. Through these studies the mechanism of interaction of drug molecules with BSA has been evaluated.

MATERIALS AND METHODS

Materials

All reagents are of analytical grade and purchased used as such as without further purification. Throughout the procedure double deionized water (with a measured resistivity of 18.2MΩ cm−1) was used.

Methodology

Azabicycle derivatives: Azabicyclononane (*2,4-Diaryl-6,7-benzo-3-azabicyclo[3.3.1]nonan-9-ones*) derivatives were synthesized chemically through Mannich reaction. These derivatives have been synthesized by Prof. Sathiyanarayanan Kulathu Iyer, Organic chemistry department VIT University Vellore [1].

BSA: BSA was procured from Sigma-Aldrich, Bangalore, India with 99% purity and was used. The stock solution of the protein was prepared in 10mM sodium phosphate buffer solution of pH 7.4 (stored at 4°C). Entire samples were prepared in 10mM phosphate buffer solution at pH 7.4.

BSA with ABN suspension: Various concentrations of ABN (6.25, 12.5, 25, 50 and 100 µM) was suspended in phosphate buffer and sonicated to obtain a homogenous suspension. BSA of concentration (10µM) in phosphate buffer was used. A mixture of ratio 1:1 was mixed and incubated for 60 min. This solution was further subjected to different instrumentation techniques to analyze interactions [8-12].

UV visible spectroscopy: The absorption spectra of UV visible spectroscopy have been recorded from 200-800 nm with an interval of 2 nm using a 5 nm slit-width (AU2701, Systronics Inc., India). Phosphate buffer was taken as a blank and was subtracted from the absorption spectra of the relevant samples to correct the influence of the background. The peak exists close to 280 nm. Various concentrations (6.25, 12.5, 25, 50 and 100µM) of ABN (5a, 5b and 5d) and BSA (10 µM) was taken (Figures 2a-2c) [13-26].

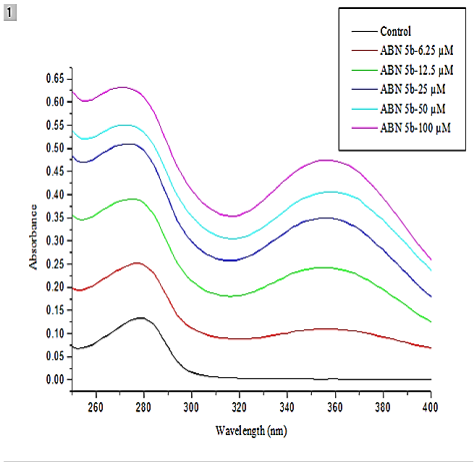

Figure 2a. Represents absorption spectra of BSA (10 µM) with ABN derivative (5a), concentration

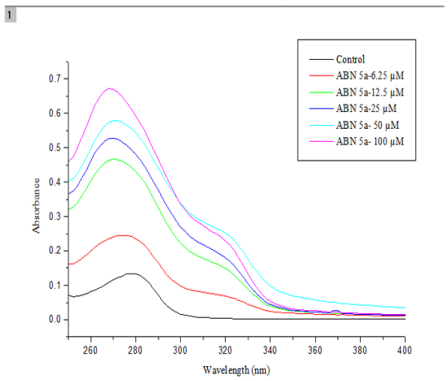

Figure 2b. Represents absorption spectra of BSA (10 µM) with ABN derivative (5b)

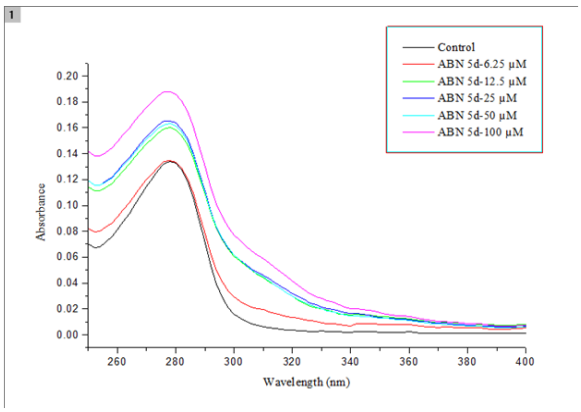

Figure 2c. Represents absorption spectra of BSA (10 µM) with ABN derivative (5d) at concentrations of 0, 6.25 µM, 12.5 µM, 25 µM, 50 µM and 100 µM in 10mM phosphate buffer (pH 7.4). There is a shift in peak with increase in ABN drug

Dynamic Light Scattering

ABN-BSA interacted complex were analysed by dynamic light scattering (DLS, ZetaSizer; HORIBA Instruments Pvt Ltd, Singapore) by making a clear and uniform suspension as described. The scattering angle was kept at 173° with holder temperature of 25.2 °C, monodispersion medium viscosity of 1.000 mPa·s, and count rate of 1247 kcps. The analyzer used was HORIBA SZ-100 for windows [Z Type] version 2.0. It can be noted that the ABN stock suspension (12.5µM) was added to the protein stock solution (10µM) in the ratio of 1:1. The measurements were taken in triplicates [27].

Fluorescence Quenching

The interaction between ABN and BSA was studied by fluorescence measurements on a HITACHI F-7000 fluorescence spectrophotometer (Tokyo, Japan) with the use of a 1.00cm path length rectangular quartz cell, wavelength range of 300-500 nm was considered to record the spectra upon excitation at 280nm, using 10 nm/10 nm slit widths, and each spectrum was an average of two scans. BSA concentration was set to be 10µM and ABN concentration ranged from 6.25µM to 50µM with an increasing order of 6.25µM. Blanks corresponding to the DI water were subtracted from the sample spectra to correct the fluorescence background before performing the analysis. Duplicate experiments were conducted for each ABN-BSA concentration.

FTIR (Fourier-Transform-Infrared) Spectroscopy

For FT-IR analysis, various concentration 12.5 µM of ABN was dispersed in DI water and was added to BSA (10µM dissolved in DI water. After 60 min incubation, 1.5ml of samples were freeze dried using lyophilizer (Scanvac Cool 110-4, Labogene, Denmark) and the lyophilized powder was analyzed using FT-IR spectroscopy (Nicolet 6700 FT-IR Spectrometer, ThermoScientific Instruments Groups, Madison, Wisconsin) in diffuse reflectance mode. Changes in the protein secondary structure were analyzed by comparing the FT-IR spectral data of the test sample (BSA-ABN suspension) with a control sample (BSA) [28].

RESULTS AND DISCUSSION

UV Visible Spectroscopy

UV visible absorption spectroscopy is the most extensively used method for determining the interaction between small molecules and protein molecules. BSA has two absorption peaks one peak exists between 200-230 nm and

other peak in 260-300nm due to p-p* transition of aromatic amino acids (tryptophan, tyrosine and phenylalanine) [8]. Figure 2 depicts the UV Vis absorption spectra of ABN-BSA, where the ABN (5a, 5b and 5d) possess maximum absorption in 280 nm. The absorption spectra of BSA and ABN show decrease in the intensity as the concentration of ABN increases. Drug binding to BSA altered the conformational changes where the peptide strands are extended and this interaction can be electrostatic or other forces such as vanderwaal's or hydrophobic interaction.

Dynamic Light Scattering

In general, DLS found to measure translational diffusion constant of the particles inside. The most basic case was that software application of Stokes-Einstein equation, assuming the ABN molecules to be spherical in size, to deduce the particle radius. Particularly, because of the presence of complex structure and the dimensional difference in BSA, that is it does not have a rotational symmetry, and which ultimately is the reason for two different coefficients for BSA, the translational diffusion coefficient and rotational diffusion coefficient [9,10]. This difference in symmetry and coefficients is the reason to get two peaks in case of protein and other bio-complexes [11,12]. When BSA dissolved in water, it exists as polymeric or unpolymeric forms.

During DLS analysis, the average size of BSA was estimated to be 53.9 nm with two different peaks observed in the range of less than 10 nm and more than 90 nm. As BSA can exist in the form of monomer or oligomer when it is in solution state, furthermore observations were in line with the previous reports [14].

It is observed that in the case of ABN-BSA interaction, both of the size distribution peaks has been merged and which shows an increase in the average size in the interacted form. Change in diameter (ΔD) can be defined as the difference between the average diameter of BSA and an average diameter of the ABN-BSA in interacted form, but in this analysis ΔD was found to be 319.7 nm, 1893.1 nm and 1893.1 nm for azabicycle derivative 5a, 5b and 5d respectively. The larger value of the chemical compound can be attributed to the fact that smaller sized ABN or better interactive capability of it which was established in earlier work [14].

It is possible that the disruption of the secondary structure of BSA molecules by ABN and numbers of factors are responsible for the degree of change including type of a protein, surface physicochemical properties of a protein and finally shape and size of the chemical compounds (Figures 3a-3d).

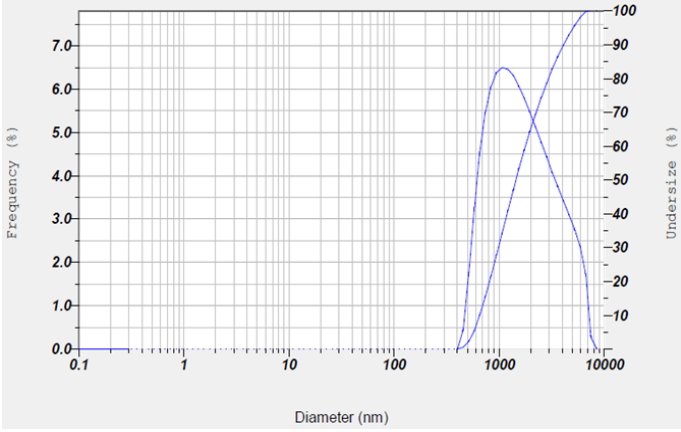

Figure 3a. Shows the peaks for BSA

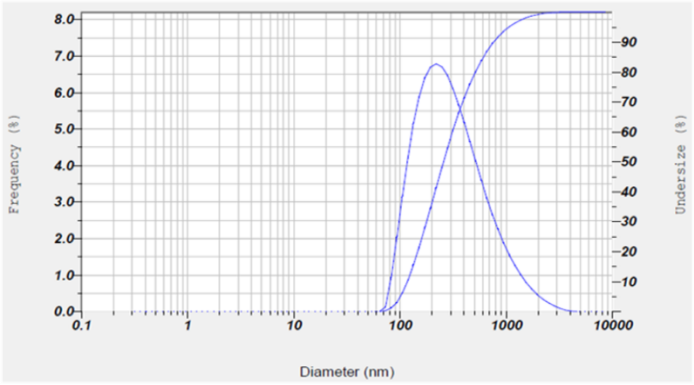

Figure 3b. Shows the peaks for ABN (5a)

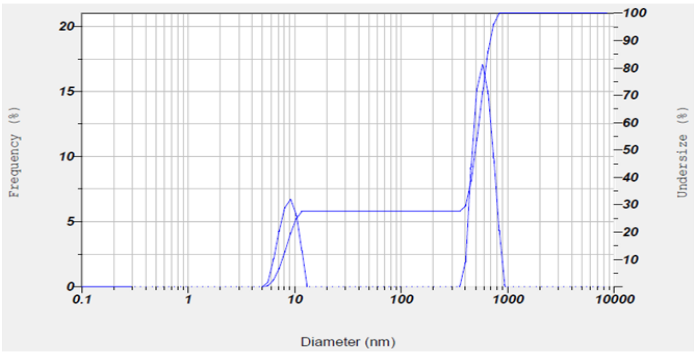

Figure 3c. Shows the peaks for ABN (5b)

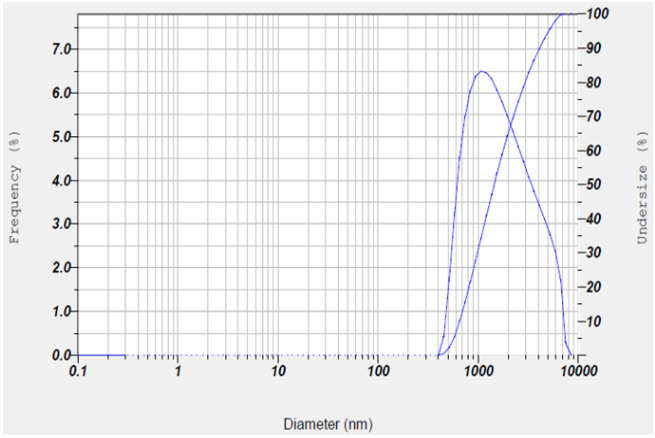

Figure 3d. Shows the peaks for ABN (5d)

ABN-BSA Interaction Analysis by Fluorescence

BSA is fluorescent in nature as it possesses tryptophan residues Trp-134 and Trp-212 in the first and second domain respectively [15]. BSA fluorescence spectra showed emission in the UV region. Interaction of ABN molecule with BSA cause change in the relative occupation of tryptophan residue and hence the protein conformation has changed. The study on fluorescence emission of BSA-ABN system was measured at a pH of 7.4 the effect of ABN on the fluorescence of BSA is shown in Figure 4a. The emission band intensity at 345nm decreases with the increasing concentration of ABN derivatives. This indicates the interaction between the drug molecules and BSA may result in variation of protein conformational changes or direct quenching effect of drug molecules [16]. Though, the

maximum emission wavelength of BSA changed through the interaction. Similar to this observation, chemically synthesized compounds of pyrimidin-5-one derivatives and BSA interaction has been performed [29].

Finally, it can be predicted that the drug mainly binds with the two fluorophores Trp-212 buried inside and Trp-134 [15] located on the surface of BSA, indicating that Trp-212 located within a hydrophobic binding pocket of BSA is not exposed to any change in polarity [17]. Trp-134 is located in this subdomain region would probably place it in the hydrophobic packing interaction between helices and close to the "distal" opening of the IB site. Protein conformation studies have confirmed that the BSA quenching property is because of the presence of TRP-134 irrespective of Trp-212, which is closely packed within BSA.

Markedly, the excitation peak between 300-400 nm gradually decreases on increasing the ABN concentration. Among the three derivatives 5d showed a high quenching intensity. The condition that attributes to ABN is masking the binding site in the region of Trp-134. Fluorescence properties was analysed in pure ABN compound and found zero sensitivity towards fluorescence. Further for ABN and BSA interaction, binding parameters were analysed by using fluorescence quenching data. The two basic mechanisms involved in quenching are dynamic and static quenching. Dynamic quenching i.e. collisional quenching occurs when excited state fluorophore is deactivated upon contact with the quencher molecule in solution. In this case, the fluorophore is returned to the ground state during a diffusive encounter with the quencher. Static quenching occurs due to the formation of a non-fluorescent ground state complex between the flurophore and the quencher. Static quenching formed due to the formation of a non-fluorescent ground state complex between flurophore and a quencher. The procedure of the fluorescence quenching was first assumed to be a dynamic quenching process. The dynamic quenching constant KSV and the apparent bimolecular quenching rate constant kq were calculated with the following Stern-Volmer equation [18].

$$\frac{F0}{F} = 1 + \mathrm{Kq}\ \text{ъo}[\mathrm{ABN}] = 1 + KSV\ [ABN]$$

Where Fo and F are the relative fluorescence intensities in the absence and presence of quencher respectively, [ABN] is the different concentration of ABN that acts as a quencher, KSV is the Stern-Volmer dynamic quenching constant, kq is the bimolecular quenching rate constant, and ъo is the average bimolecular lifetime in the absence of quencher evaluated at about 5 ns [19]. The plot of Fo/F versus [ABN] gives a straight line, and KSV is thus obtained from the slope. Plots of Fo/F versus [ABN] are shown in Figure 4b, and the calculated KSV and kq are 1.7×10^5 $M^{-1}$and $3.1 \times 101^3 M^{-1}s^{-1}$respectively. It can be noted that Kq value is much larger than the maximum scattering collisional quenching constant of various quenchers of $2.0 \times 10^{10} M^{-1}\ s^{-1}$, indicating that the probable quenching mechanism of the intrinsic fluorescence of BSA was not initiated by a dynamic process but a static quenching procedure [20]. Interestingly, the findings support the earlier findings for BSA-ABN interaction of 2,3-diazabicyclo[2.2.2]oct-2-ene (DBO) derivatives [22]. Further, to explore more the number of binding site (n) and the apparent association constant K were calculated using [21]

$$\log\left[\frac{\mathrm{F0}-\mathrm{F}}{\mathrm{F0}}\right] = \log \mathrm{K} + \mathrm{n}\log\,[\mathrm{ABN}]$$

Where, K and n are the apparent association constant and the number of binding sites respectively. Plots of log [(Fo-F)/F] versus log [ABN] are shown in Figure 4c. K and n were thus obtained from the intercept on the y-axis and the

slope respectively. The calculated K and n for ABN are 1.03 x 10^6 M^{-1} and 1.10. It can be noted that the apparent association constant depends on the concentration of ABN, temperature, and other physical parameters; it can be estimated that it also depends on the size-shape parameters of ABN which ultimately relates to the synthesis protocol followed. The medium association constants of K suggests that the affinity of ABN for BSA is high compared with the reported binding constants ranging from10^4–10^8, in which Rahman and Sharker have reported that serum albumin has a limited number of binding sites for endogenous and exogenous ligands that are typically bound reversibly [23]. The value of n is 1.1 suggesting that one or two BSA molecules bind strongly to ABN.

Additionally, Forster's theory of dipole-dipole energy transfer has been used for fluorescence resonance energy transfer analysis. The energy transfer rate depends on the extent of the overlapping of the donor emission spectrum (BSA) with the acceptor absorption spectrum (ABN), the relative orientation their transition dipoles, and the distance between these molecules. The energy transfer efficiency can be used to evaluate the distance between the ABN (acceptor) and BSA (donor) in protein by Forster's theory of dipole-dipole energy transfer as follows:

$$E = 1 - \frac{F}{F0} = [\frac{R0^6}{R0^6 + r^6}]$$

Where, and are the fluorescence intensity of BSA in the presence and absence of the acceptor respectively, is the distance between the acceptor and donor, is the critical distance for 50% energy transfer which can be calculated using the following:

$$R0^6 = 8.8X10^{25}K^2N^{-4}\,\Phi J$$

Where, the spatial orientation factor of the dipole K2=2/3, the refractive index of medium N = 1.36, and the fluorescence quantum yield of donor Φ=0.15. J can be evaluated by the overlap of the UV absorption spectra of acceptor with the fluorescence emission spectra of the donor is the overlap integral of fluorescence emission spectrum of donor and absorption spectrum of acceptor J is given by the following equation

$$J = \frac{\sum F(\lambda)\varepsilon(\lambda)\lambda^4\Delta\lambda}{\sum F(\lambda)\Delta\lambda}$$

Where the fluorescence intensity of the donor at wavelength and the molar absorption coefficient of the acceptor at wavelength. The value of r was calculated to be 1.71 nm which is less than the average distance of 2–8 nm between a donor and acceptor, indicating that the energy transfer occurred between BSA and ABN with great possibility [24]. Lesser value of r than the average distance of donor and acceptor signifies more stable and efficient interaction between ABN and BSA.

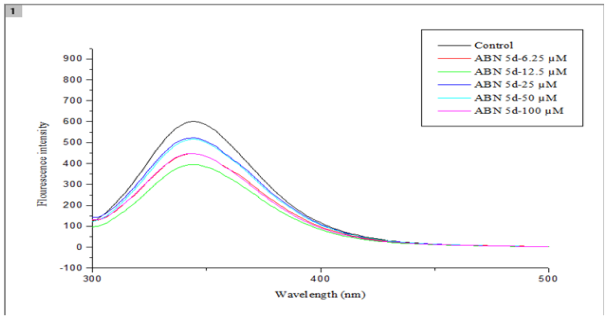

Figure 4a. Interaction between BSA and ABN as analyzed by fluorescence quenching (a) The fluorescence spectra of BSA (10 µM) and ABN (5d) at concentrations of 0 (Only BSA), 6.25 µM, 12.5 µM, 25 µM, 50 µM and 100 µM in 10 mM phosphate buffer (pH 7.4)

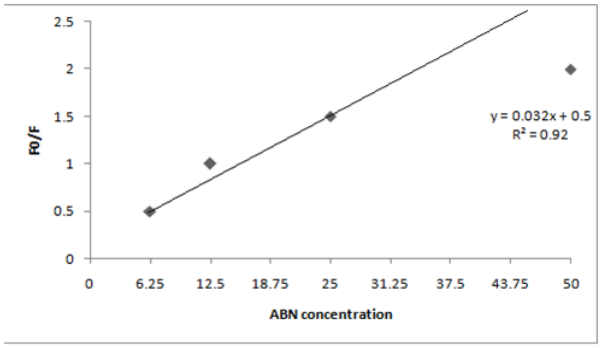

Figure 4b. Stern-Volmer plot of the fluorescence quenching of BSA (10 µM) with various concentration of ABN (5d)

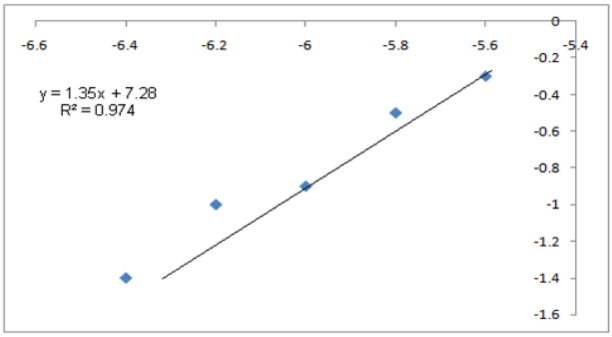

Figure 4c. Logarithmic plot of the fluorescence quenching of BSA (10 µM) with various concentration of ABN.

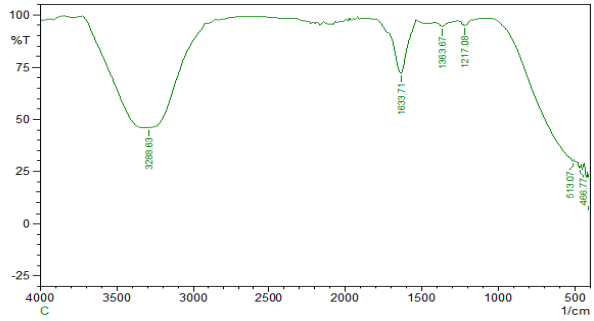

Figure 5a. FT-IR spectra of (a) native BSA (10 µM) in aqueous solution

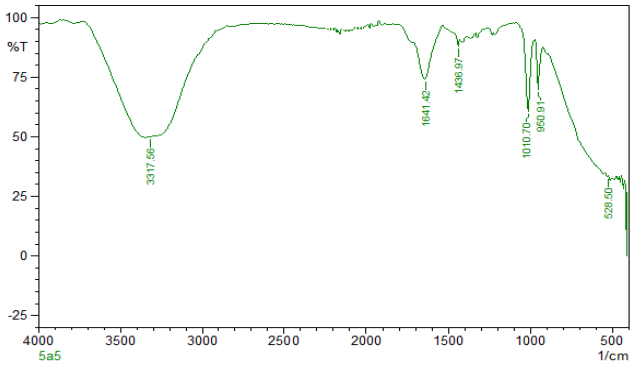

Figure 5b. interaction of BSA (10 µM) and ABN 5a (12.5 µM)

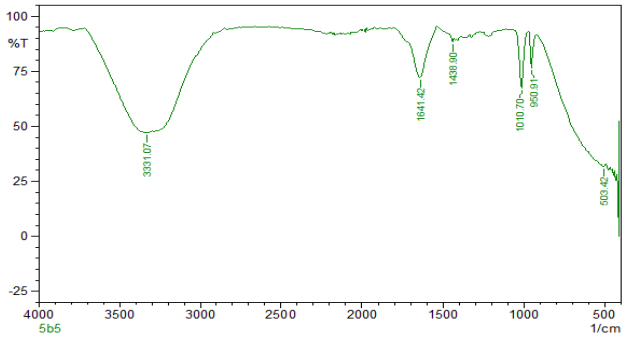

Figure 5c. interaction of BSA (10 µM) and ABN 5b (12.5 µM)

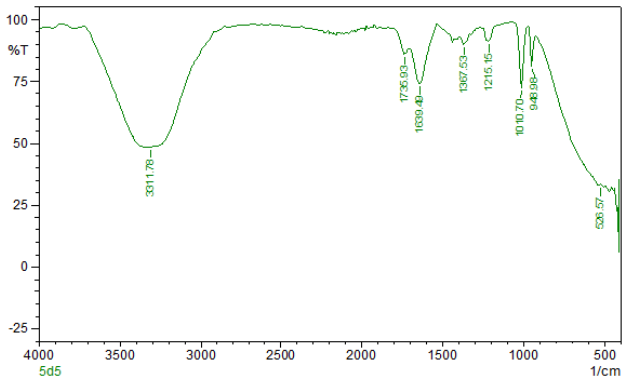

Figure 5d. interaction of BSA (10 µM) and ABN 5d (12.5 µM) in aqueous solution

ABN-BSA Interaction Analysis by FT-IR

BSA secondary derivative FT-IR spectrum is represented in Figure 4a. Usually, the amide I peak for BSA occurs in the region of 1600–1700 cm^{-1} and amide II band near 1548 cm^{-1} [25]. Amide I bands in the spectral range of 1620-1640cm^{-1} with proteins can contribute to exposed α-helix structure. As shown in Figure 4a, BSA demonstrated an exposed α-helix peak at 1633.71 cm^{-1} without the presence of ABN which is a region of amide I of BSA.

In the presence of ABN (5a), the exposed α-helix peak was found to be shifted from the original 1641.78 cm^{-1} (Figures 5a-5d) and the spectra depict a distinct peak at 1436.97 cm^{-1} which corresponds to β-sheet. However, in the ABN-BSA complex, the peak shifted to 1436.97 cm^{-1}. In same ABN (5b) second derivative the exposed α-helix peak was found to be shifted to 1641.78 cm^{-1} and peak which corresponds to β-sheet was found in 1438.90 cm^{-1}.

Further ABN (5d) the third derivative the exposed α-helix peak was found to be shifted to 1641.78 cm^{-1} and peak which corresponds to β-sheet was found in 1367.53 cm^{-1}. This implies that the protein native structure is altered which further may lead to differ the functionality and structural changes in the cell membrane. This shift in α-helix peak and in β- sheet characteristic also suggest that the BSA protein secondary structure getting distorted and the protein adsorbs to the compound through the exposed α-helices and β sheets [25]. Notably, many FTIR studies have been done with novel compounds [30] but no earlier work have been found - according to our literature survey - to analyze the ABN-BSA interaction using FTIR. BijayaKetanSahoo and co-workers have studied Azabicyclononane similar structured compound curcumin and BSA interaction by using FTIR and have observed shift in α-helix [31]. This peak shift was found lesser than the observation in ABN and BSA interaction.

CONCLUSION

Azabicycle and its derivatives are used as building blocks of fine chemicals and pharmaceuticals. Azabicycle derivatives itself a piperidone derivative and acts as a building block for drug molecules. These derivatives influence the cellular uptake, inflammation, accumulation and the bio-reactivity of a drug compound. In the present manuscript, we used ABN and BSA as a tool to understand the mechanism of protein interaction with our ABN compound. Our data showed an increase in the particle size upon interaction which suggests the conjugation of ABN with BSA. Additionally, the Stern-Volmer plot showed the static quenching in the fluorescence of BSA with increasing concentration of ABN, proved the binding of one or two protein molecules with ABN. Also, loosening of the native structure of the protein with exposed hydrophobic amino acids was observed by FTIR. Understanding the dynamics of this ABN protein interaction provides useful insights for developing and redesigning safer and value added pharmaceuticals for future applications. Detailed understanding of such interactions may lead to design biocompatible drug molecules with controlled surface characteristics in a biological environment.

ACKNOWLEDGEMENTS

Authors are thankful for the Vellore Institute of Technology (VIT, Vellore) for providing the research seed fund and providing lab facilities to carry out the present work.

REFERENCES

[1] NS Karthikeyan; G Ramachandran; KI Sathiyanarayanan; P Giridharan; PS Suresh; M Suresh Kumar; V Kasi sankar. *Journal of Pharmacy Research.* **2012**, 5(5), 2959-2964.

[2] KJ Goodall; MA Brimble; D Barker. *Tetrahedron*. 2012, 68, 5759-5778.

[3] J Hammerova; S Uldrijan; E Taborska; I Slaninova. *Journal of Dermatological Science*. **2011**, 62, 22-35.

[4] RR Luedtke; RA Freeman; VA Boundy; MW Martin; Y Huang; RH Mach. *Synapse*. **2000,** 38, 438-449.

[5] BX Huang; HY Kim. *J Am Soc Mass Spectrum.* **2004**, 15, 1237-1247.

[6] MK Prashanth; M Madaiah; HD Revanasiddappa; KN Amuruthesh. *Organic chemistry*. **2013**, 1-12.

[7] DC Carter; JX Ho. *Advances in Protein Chemistry*. **1994**, 45,153-203.

[8] JH Shi; J Chen; J Wang; YY Zhu. *Acta Part A Mol. Biomol Spectrosc.* **2015**.

[9] S Fujime; K Kubota. *Biophys Chem.* **1985**, 23, 1-13.

[10] J Rodríguez-Fernández; J Perez-Juste; LM Liz-Marzan; PR Lang. *J Phys Chem C.* **2007**, 111, 5020-5025.

[11] AK Wright; MR Thompson. *Biophys J.* **1975**, 15, 137.

[12] D Nandita; R Shivendu; D Patra; P Srivastava; A Kumar; C Ramalingam. *Chem Biol Interact.* **2016**, 253, 100-111.

[13] VM Manikandamathavan; T Weyhermuller; RP Parameswari; M Sathishkumar; V Subramanian; BU Nair. *Dalton Trans.* **2014**, 43, 13018-13031.

[14] NS Karthikeyan; SK Iyer; PG Aravindan. *Bull Korean Chem Soc.* **2009**, 30 (11), 2555-2558.

[15]K Ray; H Szmacinski; JR Lakowicz. *Anal Che.* **2009**, 81, 6049-6054.

[16] J Mariam; PM Dongre; DC Kothari. *J Fluoresc.* **2011**, 21, 2193-2199.

[17] S Dubeau; P Bourassa; TJ Thomas; HA Tajmir-Riahi. *Biomacromolecules.* 2010, 11, 1507-1515.

[18] M Yuan; R Zhong; X Yun; J Hou; Q Du; G Zhao. *Luminescence*. **2015**.

[19] X Shi; D Li; J Xie; S Wang; Z Wu; H Chen. *Chinese Sci. Bull.* **2012**, 57, 1109-1115.

[20] A Sułkowska; M Maciazek; J Równicka; B Bojko; D Pentak; WW Sułkowski. *J Mol Struct.* **2007**, 834-836, 162-169.

[21] M Xu; ZR Ma; L Huang; FJ Chen; Z Zeng. *Acta Part A Mol Biomol Spectrosc.* **2011**, 78, 503–511.

[22] S Roy; TK Das. *J Nanosci Nanotechnol.* **2014**, 14, 4899-4905.

[23] AA Rahman; SM Sharker. *Saudi Pharm J.* **2009**, 17, 249-253.

[24] N Ibrahim; H Ibrahim; S Kim; JP Nallet; F Nepveu. *Biomacromolecules.* **2010**, 11, 3341-3351.

[25] A Rajeshwari; S Pakrashi; S Dalai; Madhumita; V Iswarya; N Chandrasekaran. *J Lumin.* **2014**, 145, 859-865.

[26] D Nandita; R Shivendu; D Patra; P Srivastava; A Kumar; C Ramalingam. *Chem. Biol. Interact.* **2016**; 253: 100–111.

[27] R Huang; RP Carney; K Ikuma; F Stellacci; BLT Lau. *ACS Nano.* **2014,** 8, 5402-5412.

[28] S Ranjan; N Dasgupta; P Srivastava; C Ramalingam. *Journal of Photochemistry and Photobiology.* **2016**.

[29] S Gaonkar; Manjunath; Sunagar; N Deshpande. *Journal of Talibah University for Science*. **2018**, 12.

[30] MM Abu Teir; J Ghithan; MI Abu-Taha; SM Darwish; MM Abu-hadid. *Journal of Biophysics and structural biology.* 2014. 6.

[31] BK Sahoo; KS Ghosh; S Dasgupta. *Biophysical Chemistry.* **2008**. 132.